

**Living on the edge: biofilms developing in oscillating environmental conditions**

Sergey Dobretsov<sup>1, 2\*</sup>, Raeid M. M. Abed<sup>3</sup>, Thirumahal Muthukrishnan <sup>1, 3</sup>, Priyanka Sathe<sup>1</sup>,  
Laila Al-Naamani <sup>1</sup>, Bastien Y. Queste<sup>4</sup>, Sergey Piontkovski <sup>1</sup>

<sup>1</sup>Marine Science and Fisheries Department, College of Agricultural and Marine Sciences,  
Sultan Qaboos University, Oman

<sup>2</sup>Center of Excellence in Marine Biotechnology, Sultan Qaboos University, Oman

<sup>3</sup> Department of Biology, College of Science, Sultan Qaboos University, Oman

<sup>4</sup> Centre for Ocean and Atmospheric Sciences, University of East Anglia, Norwich NR4 7TJ,  
UK

Corresponding author:

\* Email [sergey@squ.edu.om](mailto:sergey@squ.edu.om), telephone +968 24143750; fax + 96824413418

orcid.org/0000-0002-1769-6388

## **Abstract**

For the first time, densities and diversity of microorganisms developed on the ocean glider were investigated using flow cytometry and Illumina MiSeq sequencing of 16S and 18S rRNA genes. Ocean gliders are autonomous buoyancy-driven underwater vehicles, equipped with sensors continuously recording physical, chemical, and biological parameters. Biofilms on the glider were exposed to periodical oscillations of salinity, oxygen, temperature, pressure, depth and light, due to periodic ascending and descending of the vehicle. Among the unpainted surfaces, the highest microbial abundance was observed on the bottom of the glider's body, while the lowest density was recorded on the glider's nose. Antifouling paints had the lowest densities of microorganisms. Multidimensional analysis showed that microbial communities formed on unpainted parts of the glider shared some similarity with non-toxic paint but they were significantly different from ones on toxic antifouling paint and seawater.

Keywords: biofilm, antifouling, chitosan, next generation sequencing, ocean glider, Indian Ocean.

## Introduction

Ocean gliders are a relatively recent tool in oceanography, which allow autonomous collection of long-term oceanographic data over long distances (Figure 1A). Ocean gliders are autonomous buoyancy-driven autonomous underwater vehicles (AUV), equipped with sensors continuously recording physical, chemical, and biological parameters. Compare to other AUV, the lithium sulfur chloride battery enables ocean gliders to be operational for up to 10 months and powers different sensors that can be directly controlled by an operator. The examples of sensors typically installed on ocean gliders include temperature, salinity, oxygen and chlorophyll sensors (Eriksen 2001). During the collection of the data, ocean gliders can dive from the surface to the sea bottom through changes in their buoyancy (Figure 1B). At such times, the glider and, in particular, its sensors may be vulnerable to transient biofouling. Intensity of biofouling on ocean gliders depends on the environment (Lobe et al. 2010). Generally, more organisms accumulate on surfaces in tropical waters compare to temperal ones (Moline and Wendt 2011).

Marine biofouling is the undesirable growth of organisms on submerged surfaces (Wahl 1989). Any clean artificial substrata will be colonized by bacteria and later by diatoms and other microscopic unicellular eukaryotes within hours after submersion (Salta et al. 2013). At this stage, a well-developed biofilm will be formed composed of multiple species of prokaryotic and eukaryotic organisms with dominance of bacteria and diatoms (Dobretsov 2010).

Biofouling has huge economic impacts on maritime industries. Worldwide, countries spend billions of dollars in order to manage and prevent this problem (Callow and Callow 2011). Biofouling may significantly increase vehicle drag of the ocean glider, interfere with the stability of the scientific sensors and limit good data collection (Davis et al. 2003; Medeot et al. 2011). In order to prevent biofouling, maritime industries use biocides or other toxic compounds applied as antifouling paints (Yebra et al. 2004; Lobe et al. 2010). Biocidal paints kill marine organisms and cause undesirable environmental impacts, hence new low toxic and non-toxic antifouling paints are urgently needed.

In this regard, chitosan has been proposed as a promising non-toxic antifouling agent (Pelletier et al. 2009) due to its antimicrobial properties (Kim and Rajapakse 2005). Chitosan is a naturally occurring linear polysaccharide composed of D-glucosamine and N-acetyl-D-

glucosamine obtained by deacetylation of crustacean waste (Xiao 2012). Our previous laboratory and mesocosm experiments showed that chitosan led to a reduction of densities of diatoms and bacteria on experimental paints (Al-Naamani et al. 2017). Another study demonstrated that chitosan-based paints reduced growth of bacteria for 4 days and inhibited densities of photosynthetic organisms for 14 days in northern estuarine waters (Pelletier et al. 2009). Antifouling properties of chitosan have not been studied in long-term field marine experiments in tropical waters.

The Sea of Oman, previously known as the Gulf of Oman, is situated between the shallow, (less 50 m) high salinity waters of the Arabian Gulf and the deeper (>1000 m) Arabian Sea, and hence possesses a unique hydrological regime (Al-Hashmi et al. 2010; Banse 1997; Vic et al. 2015). One of the most intensive coastal upwelling phenomena in the world characterizes Oman coastal waters (Reynolds 1993; Al-Hashmi et al. 2010). The circulation is driven by reversing summer and winter monsoons, impacting the depth of high salinity Persian (Arabian) Gulf outflow water and exchanging at the eastern boundary with the Arabian Sea (Vic et al. 2015). The unique circulation and high production in the Sea of Oman create an oxygen minimum zone where there is almost no oxygen in the water column ( $< 2 \mu\text{mol kg}^{-1}$ , Banse and Piontkovski 2006; Piontkovski et al. 2017). The Sea of Oman provides a unique opportunity to investigate formation of microbial biofilms on ocean gliders at the gradients of salinity, temperature, oxygen and pressure.

In this study, we investigated the formation of microbial biofilms on coated and uncoated parts of an ocean glider during its deployment in the Sea of Oman. Biofilms developed on the glider over 3 months and were exposed to continuous variations of salinity, oxygen, light, temperature and pressure. The main objectives of this study were to investigate: 1) the composition of prokaryotic and eukaryotic communities formed on painted and unpainted parts of the glider, and 2) the antifouling effect of commercial and non-toxic experimental paints.

## **Material and methods**

### *Ocean glider's deployment*

A Kongsberg ocean glider was deployed 5km off the coast of Muscat, Oman, at 23°41.66'N, 58°40.7'W (Figure 1C) on 4<sup>th</sup> of March 2015 and was retrieved on 3<sup>d</sup> of June 2015 (at 23°43.01'N, 58°39.7'W). The intention was to collect data throughout the end of the North-

East monsoon and the onset of the spring inter-monsoon period. The ocean glider consisted of an aluminium pressure hull surrounded by a flooded fiberglass fairing. The body of the instrument was not coated with any specific antifouling agents. Yellow coloured fiberglass maximises durability and visibility of the glider at the sea. A total of 712 dives with 1424 vertical profiles of environmental parameters covering over 2080 km and repeating the survey transects 24 times out over a period of 91 days were carried out. The ocean glider was equipped with a Seabird free-flushing CT sail, an Aanderaa 4330F oxygen optode, a Biospherical QSP-2150 PAR sensor (spectral region - 400-700 nm), a Wetlabs Triplet ECO sensor measuring chlorophyll *a* (based on fluorescence intensity) and backscatter at 470 and 700 nm (Piontkovski et al. 2017). Satellite communication was used for retrieval of the data in near real time after every dive at a speed of about 25 cm s<sup>-1</sup>.

### *Paints*

In total, five different coatings were tested (Table 1). These include two types of biocidal antifouling paints (International Micron Extra YBA 920 and Hempel Olympic 86950, later “paint”, PIn and PHe), one experimental non-biocidal chitosan paint (later “paint”, PCh) and two primer base (Intershield 300 and Hempel primer, later “base”, BIn and BHe). Base did not contain biocides and served as controls for antifouling paints. Chitosan paint was prepared according to Al-Naamani et al. (2007). Briefly, chitosan paints were made using 1.5% chitosan (Sigma Aldrich, UK) solution in 1% acetic acid (Sigma Aldrich, UK). The solution was mixed for 10 min and then sonicated for 15 min. The fibreglass surface of the glider was not protected with any specific antifouling agents (later “unprotected”, U). Before application of paints, the surface of the ocean glider was cleaned with ethanol (96%, Sigma, USA). All paints were applied in strips (10 x 70 cm) at the top and bottom of the ocean glider using brushes. The paints were air dried at room temperature for 24h before the glider was deployed into the sea.

### *Sampling*

On 3<sup>d</sup> of June 2015, the ocean glider was gently lifted to the surface of the Research Vessel Al Jamiya, Muscat, Oman. Biofilms from the painted area ~700 cm<sup>2</sup> (paint and base, Figure 1D) were scraped off using sterilized microscope slides and collected into individual sterile tubes. Remaining biofilms were washed with sterilized seawater and collected into the same

tube. Replicated samples of undisturbed biofilms were scraped off as described above from unprotected parts of the ocean glider covering an area of ~500 cm<sup>2</sup>: top (UGT) and bottom (UGB) of the body, and the top of the wings (UWT) (Figure 1D, Table 1). Biofilms from the bottom parts of the wings were disturbed during withdraw of the ocean glider and, thus, were not sampled. The smaller areas (~100 cm<sup>2</sup>) were also sampled as described above from the glider's nose (UN), the top tail wing (UTT) and the bottom tail wing (UTB) (Figure 1D). Additionally, one-litre seawater samples (seawater) were collected on 3<sup>d</sup> of June 2015 from the area of the ocean glider retrieval with Niskin bottles (volume 5L) from the depth 15m (SW1), 25m (SW2), 35m (SW3) and 50 m (SW4). Biofilm and water samples were immediately brought on ice to the Sultan Qaboos University laboratories and processed (see below).

#### *Sample analysis*

##### *Abundance of microbes*

Abundances of phytoplankton eukaryotes in water were determined by direct count in the Niskin bottle samples using a Zeiss inverted microscope (Germany, 50× and 100× magnification). The taxonomic composition of the phytoplankton eukaryotic community was characterised according to Piontkovski et al. (2017). Abundance of prokaryotes in each sample was estimated using flow cytometry (FC). FC measurements were performed using BD FACS Aria™ III (BD Biosciences, Franklin Lakes, NJ, USA). Before the analysis, each sample was filtered through 40 µm nylon cell strainer Falcon™ (Fischer Scientific, USA) to exclude large cells, cell clumps and detritus particles. Samples were stained with SYBR green I stain (Molecular Probes, Invitrogen, Carlsbad, CA, USA, excitation/emission wavelengths: 497 nm/520 nm; dilution 1:10,000) and incubated for 10 minutes in the dark. Each sample was divided onto three independent fractions. Thus, three independent FC readings were recorded for each sample. The average number of cells ml<sup>-1</sup> for each sample was calculated. The density of microorganisms on the surface of the ocean glider was calculated taking into account the size of sampled area and the amount of liquid used to wash it. Densities of prokaryotes in the water column at different sampling depths and on different parts of the glider were compared using factorial analysis of variance (ANOVA) using Statistica 11 (Statsoft, USA). Normality of the data was verified using the Shapiro-Wilk's W test. Post-hoc

Tukey's HSD test was used to test significance of differences between microbial abundances. In all cases, a  $p$  value < 0.05 was considered statistically significant.

#### *DNA extraction and MiSeq analyses*

The scraped samples from painted and unprotected surfaces of the glider were frozen and kept at -80° C until the analysis of microbial community composition using next generation sequencing. Prior to DNA extraction, water samples were filtrated through 0.2 µm Whatman (USA) filter. DNA from each sample from the glider and water column was extracted using a Power Biofilm (MoBio, USA) kit following the manufacturer's instructions. Purified DNAs were analysed at the Molecular Research (MRDNA) company (Shallowater, TX, USA). Illumina MiSeq was used to sequence the 16S and 18S rRNA genes. Bacterial V3-V4 regions of 16S rRNA genes were sequenced using the primers 515F (5'-GTGCCAGCMGCCGCGGTAA-3') and 806R (5'-GGACTACHVGGGTWTCTAAT-3'). Eukaryotic 18S rRNA genes were sequenced using the primers Euk7F (5'- AACCTGGTTGATCCTGCCAGT -3') and Euk570R (5'-GCTATTGGAGCTGGAATTAC-3').

Sequence data was processed using MRDNA analysis pipeline (MRDNA, Shallowater, TX, USA). In summary, sequences were joined, barcodes were deleted. Then, sequences <150bp and sequences with ambiguous base calls were removed. Sequences were de-noised. OTUs generated and chimeras were removed. Operational taxonomic units (OTUs) were defined by clustering at 3% divergence and 97% similarity. Final OTUs were taxonomically classified using BLASTn against a curated database derived from RDP II and NCBI (<http://rdp.cme.msu.edu>, <http://ncbi.nlm.nih.gov>).

Rarefaction curves and diversity indices (OTU richness, Chao-1 and ACE) were calculated using the Mothur software (Schloss et al. 2009). Statistical analysis of sequencing data was carried out using the PAST program (Paleontological Statistics, ver. 1.47, <http://folk.uio.no/ohammer/past>) and the R v.2.15.0 statistical platform using the *Vegan* package. The table containing samples by OTUs was used to calculate pairwise similarities among samples based on Bray-Curtis dissimilarity index (Clarke 1993). A multivariate analysis of all samples was performed using multidimensional scaling (MDS) based on Bray-Curtis dissimilarities as between biofouling communities developed on paint, base, unprotected and present in seawater. Ordination of the Bray-Curtis dissimilarities was performed using non-metric MDS, with 100 random restarts, taking into account the

presence/absence, as well as the relative abundance of OTUs in all samples. The MDS results were plotted in two dimensions. Analysis of similarities (ANOSIM) with Bonferroni corrected P values was carried out to test for significant differences between the defined sample groupings. ANOSIM produces a sample statistic *R*, which represents the degree of separation between test groups (Clarke 1993). Similarity percentage (SIMPER) analysis was performed using the PRIMER® software to compare microbial communities from seawater, coated with paint and base, as well as unprotected parts of the glider. OTU partitioning was used to find out the number of OTUs that are specific for each dataset in the MDS analysis and the number of shared OTUs between different datasets. This was done on OTUs datasets using Microsoft Excel and a custom R script.

## Results

### *Environmental parameters*

During the study, the ocean glider dove from the surface to a depth of 1015m. Vertical profiles of physical, chemical and biological characteristics recorded by the glider showed high variability during the study period (Supplementary Figure S1). This variation was attributed to the movement of the ocean glider and of mesoscale eddies, as well as seasonal changes.

The average seawater temperature during the period of investigation varied from 27.8° to 12.2° C (Figure S1A). As expected, the highest temperatures were recorded at the surface, while the lowest ones were measured at depth > 560m. The averaged vertical temperature profile implied that the surface mixed layer extended to ~25m and followed by the seasonal thermocline (Figure S1A). In turn, the thermocline layer was underlined by the Persian (Arabian) Gulf waters, with the core at 250m. This water mass, located between 150 and 350 m, flowed eastward.

The vertical profile of salinity differed from that of temperature (Figure S1B). The highest salinity of 36.9 ppt was recorded at the depth of ~260m, co-occurring with the Gulf outflow, while the lowest salinity was found at depth. The average salinity varied from 35.7 to 36.9 ppt during this study.

The photosynthetically active radiation (PAR) varied from 0 to 2400  $\mu\text{E m}^{-2} \text{ sec}^{-1}$ , during this study. A characteristic feature in the vertical distribution of the fluorescence intensity was the fluorescence peak observed at ~30-40m deep, persisting throughout the



deployment period (Figure S1C). This peak was formed by the phytoplankton community dominated by the dinoflagellate *Noctiluca scintillans* (see abundance of microbes).

Vertical distribution of the dissolved oxygen concentration showed a decline from saturated surface water ( $\sim 220 \mu\text{mol kg}^{-1}$ ) to near anoxic conditions in the oxygen minimum zone ( $< 2 \mu\text{mol kg}^{-1}$ ; below 400m). This pattern was interrupted by the outflow of Gulf water, injecting high salinity oxygenated water ( $\sim 140 \mu\text{mol kg}^{-1}$ ) between 150 and 350 m (Figure S1D).

#### *Abundance of microbes*

Taxonomic analysis of Niskin seawater samples collected within the layer of fluorescence peak (see Figure S1C) showed the presence of the dinoflagellate *Noctiluca scintillans*. This species made up about 90% of the total phytoplankton abundance (data are not shown). As for the upper mixed layer, processed samples showed that *Noctiluca* abundance was equal to  $\sim 120,000 \text{ cell L}^{-1}$  at the beginning of the experiment. At the end of the study, *Noctiluca* abundance became  $\sim 20,000 \text{ cell L}^{-1}$ .

The highest densities of microorganisms were recorded at a depth of 35 m, which correlated well with the presence of *N. scintillans* (Figure 2). The densities of microorganisms at the other depths were 14-fold to 23-fold lower. Densities of microorganisms on the ocean glider were significantly (ANOVA  $p < 0.05$ ) different (Figure 2). Among unprotected surfaces, the highest density of prokaryotes was observed on the ocean glider bottom (UGB) followed by the glider's wing (UWT) and the glider's top (UGT). The lowest density (HSD  $p < 0.05$ ) was recorded on the glider nose (UN). Among paints, the lowest density (HSD  $p < 0.05$ ) of microorganisms was found on PChT. The densities of microbes on the top and bottom surfaces were different (ANOVA  $p < 0.05$ ; Figure 2). There were significant differences (HSD  $p < 0.05$ ) in the densities of microbes on different bases tested; 3-fold higher densities were observed on BIn in comparison to that on BHe. The density on BIn was 1.5–2-fold lower (HSD  $p < 0.05$ ) than on the unprotected glider (UG) surfaces. The densities of microbes on antifouling paints (PInB) were 1.3-fold lower than on UGB (Figure 2). There was a significant difference between densities of microorganisms in biofilms collected from the top and the bottom of the unprotected parts of the ocean gliders (HSD  $p < 0.05$ ). Generally, the density of microbes was lower on the top of the glider

than on the bottom (Figure 2). Similarly, the density of microbes on PInT was 9-fold lower (HSD  $p<0.05$ ) than the density on the same paint located at the bottom of the glider (PInB).

### *Microbial diversity*

A total of 1,259,486 and 584,473 of 16S and 18S rDNA sequences, respectively, were obtained by Illumina MiSeq sequencing (Table 2). The lowest number of OTUs was observed on the ocean glider wing (UWT) and the highest number – on the primer BHeT (Table 2). A similar pattern was observed for Chao-1 and ACE indices. For eukaryotic communities, the highest number of sequences was found on the bottom of the ocean glider top tail (UTT), while the lowest number – on the bottom of the tail (UTB). The highest number of OTUs and the highest diversity Chao-1 and ACE indices were observed on the antifouling paint PInB and the lowest at the bottom of the glider's top tail (UTT) (Table 2).

The bacterial communities that developed on paints, base and uncoated surfaces had 1158 OTUs in common. The eukaryotic communities shared 355 OTUs (Figure 3). The highest number of unique bacterial OTUs was observed for paints, while the lowest one was found in biofilms on base. For eukaryotic communities, biofilms developed on unprotected parts of the glider had 138 unique OTUs, while the numbers of OTUs on base and antifouling paints were lower (Figure 3).

Multidimensional analysis (MDS) showed that bacterial communities formed on the ocean glider and present in seawater were different (Figure 4), which was supported by ANOSIM analysis ( $r=0.94$ ,  $p=0.006$ ). While bacterial communities formed on unprotected parts of the glider (U) shared some similarity with the base (BIn and BHe) and the experimental chitosan paint (PCh), they were different from the copper-based paints (PIn and PHe) (Figure 4). Similar tendency was observed for eukaryotic communities. MDS analysis showed that eukaryotic communities in the seawater and on the ocean glider were significantly different (ANOSIM  $r=0.62$ ,  $p>0.05$ ). Eukaryotic communities formed on unprotected and base surfaces shared some similarities, as well as communities from the base and paints.

SIMPER analysis demonstrated that bacteria belonging to genera *Dasania*, *Pantoea* and *Vibrio* contributed from 14% to 22% of dissimilarity between communities developed on the ocean glider and existing in seawater (Table 3). Additionally, bacterial communities formed on unprotected and base surfaces differed by the presence of the genera

*Exiguobacterium*. Eukaryotes belonging to Bacillariophyceae and Hydrozoa accounted for more than 21% each between communities developed on the glider and existing in seawater (Table 4). Additionally, Holozoa (Ichthyosporea) and different fungi (Agaricomycetes and Dothideomycetes) contributed for more than 10% each for dissimilarities between eukaryotic communities.

Bacteria belonging to the classes Gamma- and Alpha-proteobacteria dominated biofilms developed on the ocean glider during the experiment (Figure 5A). These were mainly represented by the genera *Vibrio*, *Pseudomonas*, *Alteromonas*, *Marinobacter*, *Dasania*, *Teredinibacter* and *Cycloclasticus* (Gamma-proteobacteria), *Pseudoruegeria*, *Parvibaculum*, *Sphingomonas*, *Hyphomonas*, *Erythrobacter* and *Tateyamaria* (Alpha-proteobacteria). The class Bacilli (mainly genus *Exiguobacterium*) was abundant on all unprotected parts of the ocean glider. Sequences belonging to chloroplasts of diatoms (Bacillariophyceae and Fragillariophyceae) were detected. There were clear difference between the compositions of bacterial communities developed on antifouling paints, base and unprotected parts of the ocean glider (Figure 5A). Copper-based antifouling paints had high (51-66%) relative abundance of Gamma-proteobacteria. Among antifouling paints, the chitosan paint (PChT and PChB) were characterized by the lower relative abundance of Gamma-proteobacteria (14-33%) and the higher relative abundance of Beta-proteobacteria (28-29%). Bacteria belonging to the genera *Dasania*, *Erythrobacter* and *Cycloclasticus* were the most common on paints containing copper. In contrast, *Ralstonia* sp. was dominant on chitosan experimental paint (PCh) and base. Among base, the high relative abundance of Beta-proteobacteria was observed on BHeT and BHeB, while the high abundance of Bacilli was observed on BInT and BInB. The bacterial genera *Pantoea* and *Exiguobacterium* were dominant on base and unprotected parts of the ocean glider. Different unprotected parts of the ocean glider had distinct communities. For example, biofilms on the wing (UWT) dominated with Gamma-proteobacteria (85%), while the lower relative abundance of Alpha-proteobacteria (7%) and Bacilli (7%) was also recorded. On the other hand, there were no Bacilli in the biofilms on the glider's nose (UN).

Eukaryotic communities on the ocean glider were highly diverse and represented by different groups of fungi, microalgae, nematodes, arthropods and hydrozoans (Figure 5B). Sequences of some macrofouling genera, such as *Megabalanus*, *Hydractinia*, *Actinostola*, *Dicoryne* were found. Additionally, sequences belonging to some planktonic species, like

*Nectopyramis* sp. (Siphonopora) were detected. Hydrozoa had high relative abundance on base (BInB 58%; BHeT 79%), the glider's nose (UN 79%) and the antifouling paint (PInB 53%). High fungal diversity (represented by 5 different classes) in marine biofilms was detected (Figure 5B). The fungal class Agaricomycetes was highly abundant (relative abundance 72%) on paint PHeT, while the class Dothideomycetes (relative abundance 46%) and Eurotiomycetes (relative abundance 14%) were highly abundant on unprotected parts (UTB). The relative abundance of the fungal class Sordariomycetes on the antifouling paint PHeB was 7%. The highest relative abundance (89%) of the class Ichtyosporea (Mesomycetozoea, Holozoa) on PInT was recorded (Figure 5B). Diatoms (Bacillariophyceae), mainly *Amphora* and *Cylindrotheca* species, dominated biofilms on the ocean glider unprotected surfaces (UWT 82% and UTT 94%), chitosan paint (PChB 71%; PChT 59%) and base (BInT 73%). More than half of the sequences (54%) obtained from the unprotected bottom of the ocean glider (UGB) belonged to Chlorophyta (*Pycnococcus* sp.).

## Discussion

This is the first study that investigated microbial fouling on the ocean glider by next generation sequencing. Previous studies reported presence of macrofouling organisms on ocean gliders (Nicholson et al. 2008; Moline and Wendt 2011), but neglected microbial biofilms, which may also affect the performance of the glider and its sensors (Davis et al. 2003; Cetinic et al. 2009).

During the study period, vertical profiles of temperature, oxygen, chlorophyll and salinity showed high variability. The study area is highly influenced by three hydrodynamical processes: (1) the outflow from the Persian (Arabian) Gulf, (2) the inflow from the northern Arabian Sea, and (3) the mesoscale (cyclonic and anti-cyclonic) eddies persisting in the region (across the Gulf) and connecting the northern-banked inflow and the southern-banked outflow (Al-Hashmi et al. 2010; Vic et al. 2015). Thus, we assume that variations of the physical and biological parameters in the study region could be attributed to the spatial shifts in the location of the mesoscale eddy affecting regional circulation over the shelf in Muscat region. Additionally, seasonal changes (i.e. increase of temperature from March to June) have affected vertical profiles of the physical and biological parameters (Piontkovski et al. 2017).

Biofilms on the surface of the ocean glider were exposed to continuous fluctuations of oxygen ( $0 - 287 \mu\text{mol kg}^{-1}$ ), temperature ( $12.2- 32.3^{\circ}\text{C}$ ), salinity ( $35.4-38.0$  ppt), depth ( $0- 1015$  m), pressure ( $0.04- 102$  Bar) and light intensity ( $0- 2400 \mu\text{E m}^{-2} \text{sec}^{-1}$ ) for more than 3 months. We expected that microbes on the glider would differ from those in the water column. Indeed, as shown by the MDS plots, the composition of bacterial and eukaryotic organisms on the ocean glider and in the water column was very different. Previously it was reported that attached and particle-bound bacteria are more abundant and more metabolically active than unattached bacteria (Kirchman and Mitchell 1982; Dang and Lovell 2016). The densities of microorganisms on the glider's surface varied from 8,820 to 228,000 cell/mm<sup>2</sup>. Among unprotected surfaces the lowest densities of microbes were found on the nose of the ocean glider (UN). Probably, it is due to the higher dynamic pressure and velocities on that part of the glider (Isa et al. 2014; Chen et al. 2015). Additionally, the densities of microorganisms on the top of the ocean glider were generally lower than on the bottom. The orientation of different parts of the ocean glider could affect the densities of microbes (Bellou et al. 2012).

Ocean glider's parts painted with antifouling paints had lower densities of microorganisms than unprotected parts of the glider. This is not surprising, as antifouling paints contain chemical compounds that kill or prevent growth of microfouling organisms (Casse and Swain 2006; Mollino et al. 2009; Briand et al. 2012; Briand et al. 2017). The lowest densities of microorganisms were observed on the antifouling paints PHeT and PHeB that contained biocides cuprous oxide and zineb. In previous studies, both biocides were recognised as effective antifouling agents (Hunter and Evans 1991). Among 11 commercial antifouling paints tested during a 1 year study in Oman coastal waters, the lowest microbial biomass was recorded on the paint with these biocides (Muthukrishnan et al. 2014).

Compared to other studies of marine biofilms on artificial surfaces utilizing the Illumina MiSeq technique, the diversity of communities formed on the ocean glider was similar to that found in Australia (Tan et al. 2015) and Swedish (Oberbeckmann et al. 2016) coastal waters. Bacteria belonging to the classes Gamma- and Alpha-proteobacteria, mostly *Vibrio*, *Pseudomonas*, *Teredinibacter*, *Cycloclasticus*, *Pseudoruegeria*, *Parvibaculum*, *Sphingomonas*, *Erythrobacter* and *Tateyamaria*, dominated in biofilms. Similarly, previous investigations demonstrated the dominance of Alpha- and Gamma-proteobacteria in marine biofilms on various artificial substrata (Dobretsov et al. 2013; Tan et al. 2015; Sathe et al.

2016; Flach et al. 2017; Hunsucker et al. 2018). Differences between bacterial communities developed on the ocean glider were due to the genera *Dasania*, *Pantoea*, *Exiguobacterium* and *Vibrio* as indicated by SIMPER analysis. *Dasania* are obligately aerobic bacteria (Lee et al. 2007), which previously found associated with the deep sea tubeworm (Forget and Juniper 2013). *Exiguobacterium profundum* was previously isolated from a deep sea hydrothermal vent (Crapart et al. 2007). This might suggest possible adaptations of these bacteria to high pressure and low oxygen conditions. Archaea dominate deep sea waters (De Long 1992; Jensen et al. 2012) but this group was not detected in this study. While the universal 16S RNA 515F/806R primers used in this research have been used to study both archaea and bacteria (Bates et al. 2010; Walters et al. 2011), it is possible that the absence of archaea in this study was due to poor amplification of this group of microorganisms (Eloe-Fadrosh et al. 2016).

Eukaryotic communities on the ocean glider were predominantly represented by fungi, hydrozoans and arthropods. While only biofilms were observed on the glider, sequences of macrofouling organisms, such as the barnacle *Megabalanus* sp. and the hydrozoan *Hydractinia* sp., might indicate recruitment of these species on the ocean glider. Barnacles are reported as the main fouling species on ocean gliders (Lobe et al. 2010). Additionally, sequences of photosynthetic species belonging to the classes Bacillariophyta, Dinophyceae, Chlorophyta and Mediophyceae were recorded. This might indicate that some photosynthetic species on the ocean glider, like *Amphora* sp. and *Cylindrotheca* sp., can sustain some time without light. It has been shown that the benthic diatoms *Amphora coffeaeformis* and *Cylindrotheca closterium* can survive in the dark, anoxic conditions for 6-28 weeks (Kamp et al. 2011). The researchers have found that these diatoms accumulated nitrate and used it for their respiration in the absence of oxygen and light.

The composition of microbial communities developed on paints, primer and unprotected parts of the glider was different. This could be explained by different chemical (chemical composition) and physical (wettability) properties of unprotected and coated surfaces. For example, biologically and physically inert substrates, like glass, fouled quicker and had more diverse communities than active substrates, like copper-nickel alloys (Marszalek et al. 1979). 454 pyrosequencing of 16S genes revealed the presence of different microbial communities on different antifouling paints (Muthukrishnan et al. 2014; Briand et al. 2017). The copper antifouling paint resulted in significant changes in both bacterial and

eukaryotic communities in New Zealand waters (von Ammon et al. 2018). Similar results were obtained in the experiments with plastic panels painted and not painted with antifouling paints in Swedish waters (Flach et al. 2017). Bacteria belonging to Cryomorphaceae and Alcanivoraceae were exclusively present on polyethylene terephthalate but not on glass surfaces in another study in the North Sea (Oberbeckmann et al. 2016). In our study, bacteria belonging to the genera *Dasania*, *Erythrobacter* and *Cycloclasticus* were common on antifouling paints containing cuprous oxide. While the genus *Dasania* was previously detected on antifouling paints, the genus *Erythrobacter* was observed in biofilms on cuprous oxide antifouling paints (Muthukrishnan et al. 2014). *Cycloclasticus* was one of the two most abundant genera in biofilms on antifouling paints exposed to fouling in Swedish coastal waters (Flach et al. 2017). This could suggest that bacteria belonging to *Dasania*, *Erythrobacter* and *Cycloclasticus* are commonly associated with antifouling paints.

Bacterial and eukaryotic communities on the chitosan paint were different from other antifouling paints. Differences in antifouling mechanisms can explain differences between community composition of chitosan and copper-based paints. Copper-based paints kill microorganisms due to the displacement of essential metals in proteins (Thurman et al. 1989). Copper ions may alter enzyme and nucleic acids structure and function, facilitate their hydrolysis and have an adverse effect on oxidative phosphorylation and osmotic balance (Borkow and Gabbay 2005). On the other hand, chitosan inhibits biofouling due to its cationic nature and interactions with positively charged microbial cell membranes (Alisashi and Aider 2012).

The current study was conducted using one ocean glider. While the replicated samples were collected, these cannot be treated as true replicates. It is partially difficult to replicate naval structures. There are several similar studies of biofilms on ship hulls that did not have true replicates (Hunsucker et al. 2014; Inbakandan et al. 2010; Zargiel et al. 2011). Gliders are expensive autonomous vehicles and cannot be easily replicated. In fact, we tried to have two independent replicates but the second ocean glider was lost during the experiment. Thus, conclusions of this study need to be treated with caution.

In conclusion, for the first time the presence of diverse microbial biofilms formed on the surface of the ocean glider exposed to oscillating environmental conditions was demonstrated using next generation sequencing techniques. Densities and compositions of

microbial communities on different parts of the glider were different, which could be explained by differences in hydrodynamic conditions on different parts of the glider. Additionally, chemical composition of unprotected surfaces and coated with base and paint shaped the composition of microbial communities on the surface of the ocean glider. This is the first attempt to investigate of biofouling on ocean gliders and much work is required in the future to confirm our findings. Differential antifouling performance of paints, suggested that proper antifouling solutions for long endurance autonomous underwater vehicles need to be developed.

## **Acknowledgements**

Ocean glider deployments were undertaken as part of the Office of Naval Research GLOBAL grant N62909-14-1-N224 (SQU EG/AGR/FISH/14/01), EG/AGR/FISH/17/01, UK NERC grants NE/M005801/1 and NE/N012658/1. SD's work was supported by the SQU grant IG/AGR/FISH/18/02 and the TRC project RC/AGR/FISH/16/01. The authors thank Dr. Gerd Bruss for his help with the data analysis.

## **Disclosure statement**

The authors declare that they have no conflicts of interest related to this work.

## **References**

- Al-Hashmi K, Claereboudt AM, Al-Azri AR, Piontkovski SA. 2010. Seasonal changes of chlorophyll "a" and environmental characteristics in the Sea of Oman. *The Open Marine Biology Journal*. 4: 107-14.
- Al-Naamani L, Dobretsov S, Dutta J, Burgess G. 2017. Chitosan-ZnO nanocomposite coatings for the prevention of marine fouling. *Chemosphere*. 168: 408-17
- Alisashi A, Aider M. 2012. Applications of chitosan in the seafood industry and aquaculture: a review. *Food Bioprocess Technol*. 5: 817e830.
- Banse K. 1997. Irregular flow of Persian (Arabian) Gulf water to the Arabian Sea. *J Mar Res*. 55: 1049-67.
- Banse K, Piontkovski SA. 2006. The mesoscale structure of the epipelagic ecosystem of the open Northern Arabian Sea. Hyderabad: Universities Press, 2006, 237 pp.
- Bates ST, Berg-Lyons D, Caporaso JG, et al. 2010. Examining the global distribution of dominant archaeal populations in soil. *ISME J*. 5: 908-917.
- Bellou N, Papathanassiou E, Dobretsov S, et al. 2012. The effect of substratum type, orientation and depth on the development of bacterial deep-sea biofilm communities grown on artificial substrata deployed in the Eastern Mediterranean. *Biofouling*. 28:199-213.
- Briand J-F, Barani A, Garnier C, et al. 2017. Spatio-Temporal Variations of Marine Biofilm Communities Colonizing Artificial Substrata Including Antifouling Coatings in Contrasted French Coastal Environments. *Microb Ecol*. 74: 585-598.



- Briand J-F, Djeridi I, Jamet D, et al. 2012. Pioneer marine biofilms on artificial surfaces including antifouling coatings immersed in two contrasting French Mediterranean coast sites. *Biofouling*. 28:453–63.
- Borkow G, Gabbay J. 2005. Copper as a biocidal tool. *Curr Med Chem*. 12: 2163–2175.
- Callow JA, Callow ME. 2011. Trends in the development of environmentally friendly fouling-resistant marine coatings. *Nat Commun*. 2:803–814.
- Cassé F, Swain GW. 2006. The development of microfouling on four commercial antifouling coatings under static and dynamic immersion. *Int Biodeterior Biodegrad*. 57: 179–185.
- Cetinic I, Toro-Farmer G, Ragan M, et al. 2009. Calibration procedure for Slocum seaglider deployed optical instruments. *Opt Express*. 31: 15420-30.
- Chen C-L, Maki JS, Rittschof D, et al. 2013. Early marine bacterial biofilm on a copper-based antifouling paint. *Int Biodeterior Biodegrad*. 83:71–76.
- Clarke KR. 1993. Non-parametric multivariate analysis of changes in community structure. *Aust J Ecol*. 18: 117-43.
- Crapart S, Fardeau ML, Cayol JL, et al. 2007. *Exiguobacterium profundum* sp. nov., a moderately thermophilic, lactic acid-producing bacterium isolated from a deep-sea hydrothermal vent. *Int J Syst Evol Microbiol*. 57: 287-292.
- Dang H, Lovell CR. 2016. Microbial Surface Colonization and Biofilm Development in Marine Environments. *Microbiol Mol Biol Rev*. 80: 91-138.
- Davis R, Eriksen C, Jones C. 2003. Autonomous buoyancy-driven underwater seaseaggliders. In: Griffiths G (Ed). *Technology and application of underwater vehicles*. London: Taylor and Francis, 37-58.
- DeLong EF. 1992. Archaea in coastal marine environments. *PNAS*. 89: 5685-5689.
- Dobretsov S. 2010. Marine Biofilms. In: Dürr S, Thomason JC (Eds). *Biofouling*. Oxford: Wiley-Blackwell, 123-136.
- Dobretsov S, Abed RMM, Voolstra CR. 2013. The effect of surface colour on the formation of marine micro- and macro-fouling communities. *Biofouling*. 29: 617-627.
- Eloe-Fadrosh E, Paez-Espino D, Jarett J, et al. 2016. Global metagenomic survey reveals a new bacterial candidate phylum in geothermal springs. *Nat Commun*. 7: 10476
- Eriksen CC, Osse TJ, Light RD, et al. 2001. Seaseaglider: A long-range autonomous underwater vehicle for oceanographic research. *IEEE Journal of Ocean Engineering*. 26:424-436.
- Forget NL, Juniper SK. 2013. Free-living bacterial communities associated with tubeworm (*Ridgeia piscesae*) aggregations in contrasting diffuse flow hydrothermal vent habitats at the Main Endeavour Field, Juan de Fuca Ridge. *Microbiology Open*. 2: 259-275.
- Flach CF, Pal C, Svensson CJ, et al. 2017. Does antifouling paint select for antibiotic resistance? *Sci Total Environ*. 590-591:461-68.
- Hunsucker KZ, Vora GJ, Hunsucker JT, Gardener H, et al. 2018. Biofilm community structure and the associated drag penalties of a groomed fouling release ship hull coating. *Biofouling*. 34: 162-172.
- Hunsucker KZ, Koka A, Lund G, Swain G. 2018. Diatom community structure on in-service cruise ship. *Biofouling*. 30: 1133-1140.
- Hunter JE, Evans LV. 1991. Raft trial experiments on antifouling paints containing zineb and copper. *Biofouling* 3: 113-137.
- Isa K, Arshad MR, Ishak S. 2014. A hybrid-driven underwater seaglider model, hydrodynamics estimation, and an analysis of the motion control. *Ocean engineering*. 81: 111-129.
- Inbakandan D, Murthy PS, Venkatesan R, Khan SA. 2010. 16S rDNA sequence analysis of culturable marine biofilm forming bacteria from a ship's hull. *Biofouling* 26: 893-899.
- Jensen S, Bourne DG, Hovland M, et al. 2012. High diversity of microplankton surrounds deep-water coral reef in the Norwegian Sea. *FEMS Microb Ecol* 82: 75-89.
- Kamp A, de Beer D, Nitsch JL, et al. 2011. Diatoms respire nitrate to survive dark and anoxic conditions. *PNAS*. 108:5949-5954.

- Kim SK, Rajapakse N. 2005. Enzymatic production and biological activities of chitosan oligosaccharides (COS): a review. *Carbohydr Polym.* 62: 357-368.
- Kirchman D, Mitchell R. 1982. Contribution of Particle-Bound Bacteria to Total Microheterotrophic Activity in Five Ponds and Two Marshes. *Appl Env Microb.* 43: 200-209.
- Lee YK, Hong SG, Chtó HH, et al. 2007. *Dasania marina* gen. nov., sp. nov., of the order Pseudomonadales, isolated from Arctic marine sediment. *J Microbiol.* 45:505-509.
- Lobe H, Haldeman C, Glenn SM. 2010. ClearSignal Coating Controls Biofouling on the Rutgers Seaglider Crossing. Arlington, VA: Compass Publications Inc, 4 pp. ISSN 0093-3651.
- Marszalek DS, Gerchakov SM, Udey LR. 1979. Influence of Substrate Composition on Marine Microfouling. *Appl Env Microb.* 38: 987-995.
- Medeot N, Nair R, Gerin R. 2011. Laboratory Evaluation and Control of Slocum Seaglider C–T Sensors. *Journal of Atmospheric and Oceanic Technology.* 28:838-846.
- Moline MA, Wendt D. 2011. Evaluation of seaglider coatings against biofouling for improved flight performance. California polytechnic state University San Luis, Biological sciences department, pp. 11. Available at <http://www.dtic.mil/docs/citations/ADA547644>.
- Molino PJ, Campbell E, Wetherbee R. 2009. Development of the initial diatom microfouling layer on antifouling and fouling-release surfaces in temperate and tropical Australia. *Biofouling.* 25:685–694.
- Muthukrishnan T, Abed RMM, Dobretsov S, et al. 2014. Long-term microfouling on commercial biocidal fouling control coatings. *Biofouling.* 30:1155–1164.
- Nicholson D, Emerson S, Eriksen CC. 2008. Net community production in the deep euphotic zone of the subtropical North Pacific gyre from seaglider surveys. *Limnol Ocean.* 53: 2226-22236.
- Oberbeckmann S, Osborn MA, Duhaime MB. 2016. Microbes on a Bottle: Substrate, Season and Geography Influence Community Composition of Microbes Colonizing Marine Plastic Debris. *PLOS One.* 3: 11(8)e0159289
- Pelletier E, Bonnet C, Lemarchand K. 2009. Biofouling growth in cold estuarine waters and evaluation of some chitosan and copper anti-fouling paints. *Int J Mol Sci.* 10: 3209-3223.
- Piontkovski SA, Queste B, Al-Shaai A, et al. 2017. Subsurface algal blooms of the north-western Arabian Sea. *Marine Ecology Progress Series.* 566: 67-78.
- Reynolds M. 1993. Physical oceanography of the Gulf, Strait of Hormuz, and the Gulf of Oman—Results from the *Mt Mitchell* expedition. *Mar Poll Bull.* 27: 35-59.
- Salta M, Wharton JA, Blache Y, et al. 2013. Marine biofilms on artificial surfaces: structure and dynamics. *Environ Microbiol.* 15: 2879–2893.
- Sathe P, Myint MTZ, Dobretsov S, Dutta J. 2016. Self-decontaminating photocatalytic zinc oxide nanorod coatings for prevention of marine microfouling: a mesocosm study. *Biofouling.* 32: 383-395.
- Schloss PD, Westcott SL, Ryabin T, et al. 2009. Introducing mothur: Open-source, platform-independent, community-supported software for describing and comparing microbial communities. *Appl Environ Microbiol.* 75: 7537-7541.
- Tan E L-Y, Mayer-Pinto M, Johnston EL, et al. 2015. Differences in Intertidal Microbial Assemblages on Urban Structures and Natural Rocky Reef. *Frontiers Microbiol.* 6: 1276.
- Thurman RB, Gerba CP, Bitton G. 1989. The molecular mechanisms of copper and silver ion disinfection of bacteria and viruses. *Critical Rev Environ Control.* 18: 295-315.
- Vic C, Roulet G, Capet X, et al. 2015. Eddy-topography interactions and the fate of the Persian Gulf Outflow. *J Geophys Res Ocean.* 120: 6700–17.
- Von Ammon U, Wood SA, Laroche O, et al. 2018. The impact of artificial surfaces on marine bacterial and eukaryotic biofouling assemblages: A high-throughput sequencing analysis. *Mar Environ Res.* 133: 57-66.
- Walters WA, Caporaso JG, Lauber CL, et al. 2011. PrimerProspector: *de novo* design and taxonomic analysis of barcoded polymerase chain reaction primers. *Bioinformatics.* 27: 1159-1161.

589 Wahl M. 1989. Marine epibiosis. I. Fouling and antifouling: some basic aspects. Mar Ecol Progr Ser .  
590 58: 175-189.  
591 Xiao C. 2012. Functionalisation and application of chitosan. In: Mackay RG, Tait JM (Eds.), Handbook  
592 of Chitosan Research and Applications. New York: Nova Science Publishers Inc., 301-313.  
593 Yebra DM, Kiil S, Dam-Johansen K. 2004. Antifouling technology- past, present and future steps  
594 towards efficient and environmentally friendly antifouling coatings. Progr Org Coat. 50: 75-104.  
595 Zargiel KA, Coogan JS, Swain GW. 2011. Diatom community structure on commercially available ship  
596 coatings. Biofouling 27: 955-965.  
597

598

## Figure legends

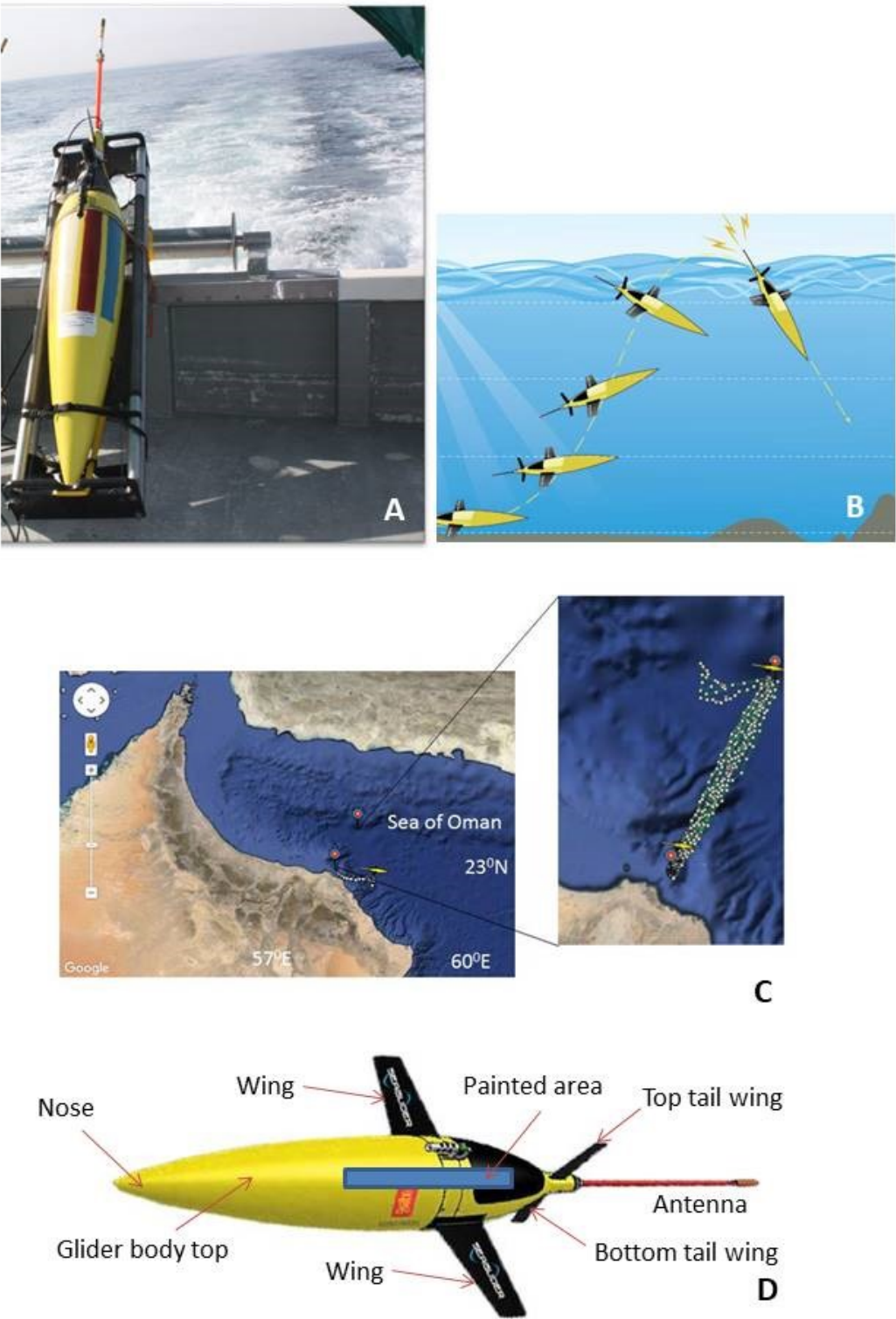
**Figure 1.** **A.** Ocean glider on the boat of the research vessel. **B.** The scheme of a glider's dive (from <http://www.kronberg.com> and <http://www.ueaseaglider.uea.ac.uk/DIVES/>). **C.** Google Map showing the sampling area. **Insert:** Location of ocean glider's transects in the Sea of Oman. **D.** The sampled locations on the glider (modified from <http://auvac.org/platforms/view/160>).

**Figure 2.** Total microbial abundance of microbial cells in seawater samples, on unprotected ocean glider surface and coated with paints and base. Data are the mean + standard deviation (SD). For the sample abbreviations, see Table 1.

**Figure 3.** Vienn diagram showing the number of shared and unique OTUs in bacterial and eukaryotic communities developed on paints, base and the glider's unprotected surface.

**Figure 4.** Multidimensional scaling (MDS) plots of bacterial and eukaryotic microbial communities obtained from seawater and developed on the ocean glider. For the codes, see Table 1.

**Figure 5.** Heat map showing the relative abundance (%) of the main **A:** prokaryotic and **B:** eukaryotic classes present in biofilms developed on the ocean glider. For the codes, see Table 1.



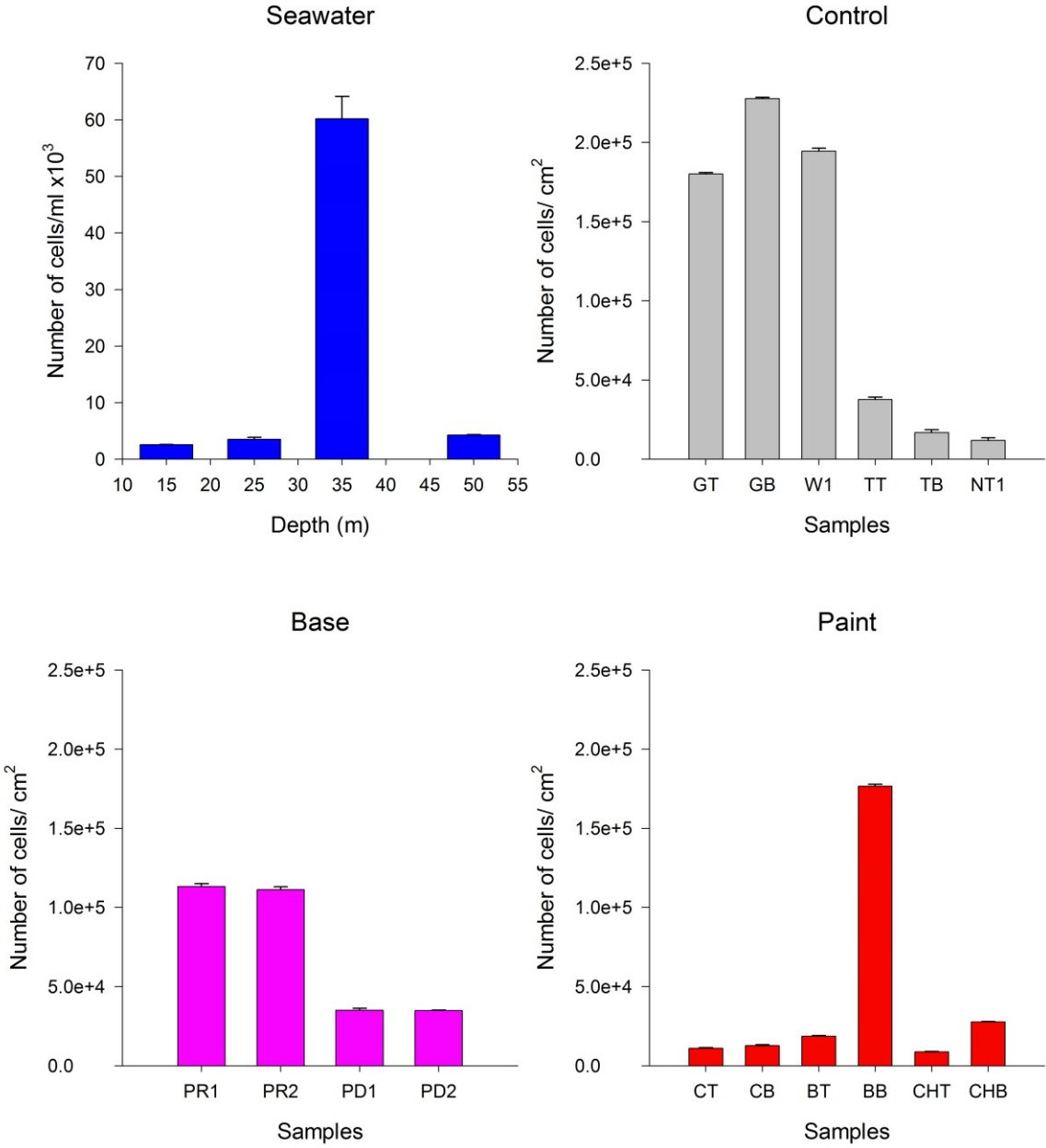
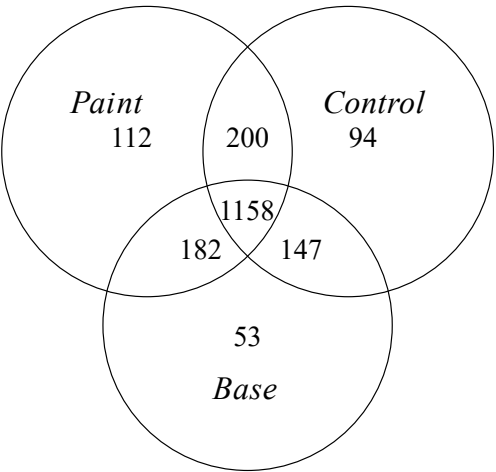


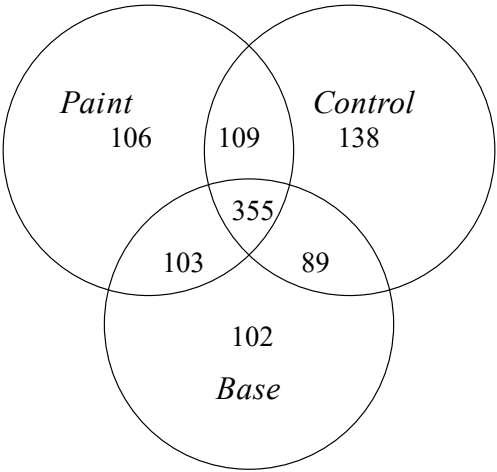
**Figure 2**

630

**Bacterial communities**



**Eukaryotic communities**



631

632

633 **Figure 3**

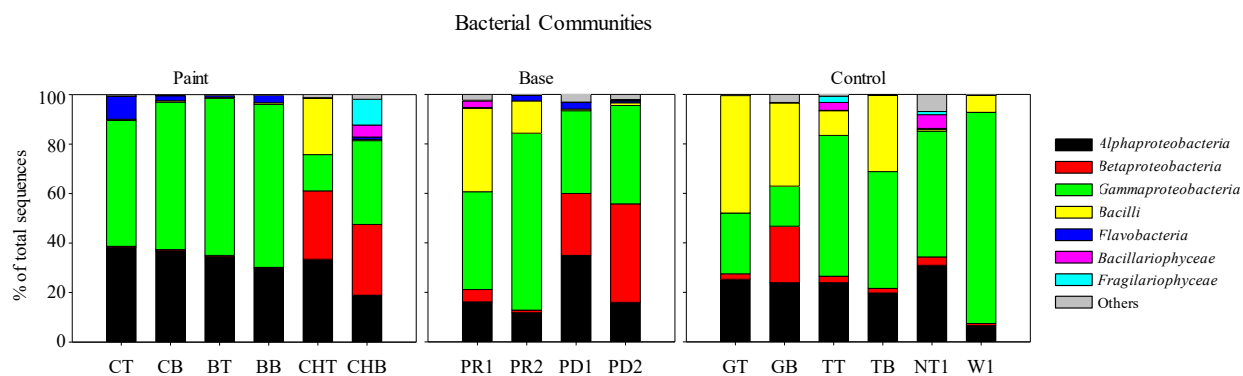
634

636  
637  
638  
639





A



B

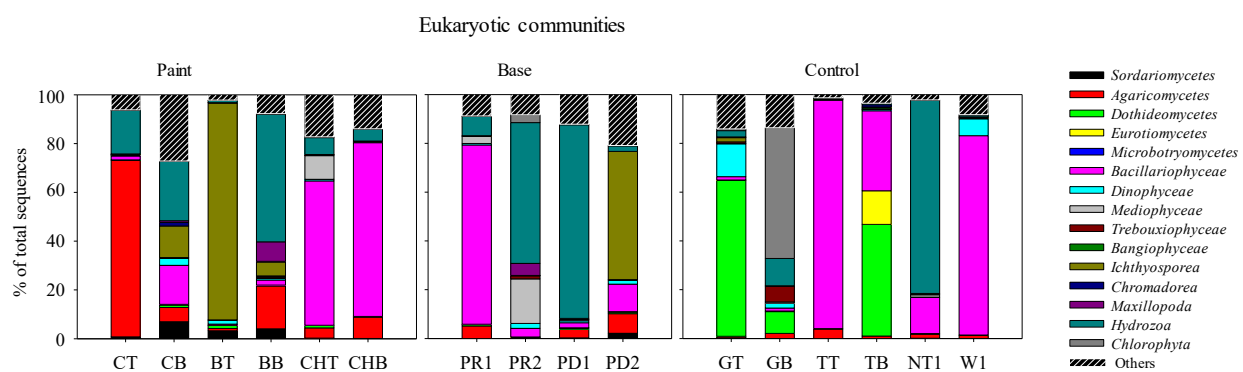


Figure 5

## Tables

**Table 1.** Samples taken from the ocean glider and characteristics of paints used in this study

Code	Treatment	Location	Paint	Type of paint	Active ingredient
PHeT	Paint	Glider top	Hempel Olympic 86950	Biocidal	Cuprouse oxide and Zineb
PHeB	Paint	Glider bottom	Hempel Olympic 86950	Biocidal	Cuprouse oxide and Zineb
PInT	Paint	Glider top	International micron extra YBA920	Biocidal	Cuprous oxide Dichlofluanid
PInB	Paint	Glider bottom	International micron extra YBA920	Biocidal	Cuprous oxide Dichlofluanid
PChT	Paint	Glider top	Experimental chitosan	Non-biocidal	Chitosan
PChB	Paint	Glider bottom	Experimental chitosan	Non-biocidal	Chitosan
BInT	Base	Glider top	Primer Intershield 300	Non-biocidal	No
BInB	Base	Glider bottom	Primer Intershield 300	Non-biocidal	No
BHeT	Base	Glider top	Hempel Primer 26050	Non-biocidal	No
BHeB	Base	Glider bottom	Hempel Primer 26050	Non-biocidal	No
UGT	Unprotected	Glider top	No	No	No
UGB	Unprotected	Glider bottom	No	No	No
UTT	Unprotected	Glider's tail wing top	No	No	No
UTB	Unprotected	Glider's tail wing bottom	No	No	No
UWT	Unprotected	Glider's wings top	No	No	No
UN	Unprotected	Glider's nose	No	No	No

**Table 2.** Amplicon library size and diversity estimators for bacterial and eukaryotic communities of the samples using MiSeq. Operational taxonomic units (OTUs) at 3% sequence dissimilarity were calculated based on equal subsets of sequences for all samples. For the codes see Table 1.

Sample ID	<i>Bacterial communities</i>				<i>Eukaryotic communities</i>			
	No.of sequences	No. of OTUs <sub>0.03</sub>	Chao-1	ACE	No.of sequences	No. of OTUs <sub>0.03</sub>	Chao-1	ACE
CT	98674	762	1093	1088	36456	195	304	308
CB	83526	707	1015	975	30834	281	404	414
BT	82157	703	1047	1024	46547	207	313	311
BB	93168	727	1059	1031	43754	313	439	449
CHT	77260	701	1059	1055	30718	241	361	396
CHB	44662	657	937	991	34850	205	325	338
GT	100276	593	931	917	30879	289	395	361
GB	101425	645	978	985	29418	228	363	344
TT	110038	605	906	904	47224	156	297	286
TB	69545	619	945	949	29047	188	283	277
NT1	62828	840	1171	1240	40020	235	345	352
W1	64661	561	946	912	36698	261	343	330
PR1	81755	660	977	986	30779	226	307	320
PR2	64634	628	957	984	45861	286	359	352
PD1	63290	879	1142	1166	36206	245	364	364
PD2	61587	766	1148	1134	35182	263	346	342

**Table 3.** The contribution of particular bacterial genera towards the total dissimilarity (in per cent) between the bacterial communities using similarity percentage (SIMPER) analysis. Groups with contribution  $\geq 2\%$  are shown.

Paint vs. Control		Paint vs. Base		Paint vs. Seawater		Control vs. Base		Control vs. Seawater		Base vs. Seawater	
Taxon	Con trb. %	Taxon	Con trb. %	Taxon	Con trb. %	Taxon	Con trb. %	Taxon	Con trb. %	Taxon	Con trb. %
<i>Dasania</i>	21.7	<i>Dasania</i>	21.4	<i>Dasania</i>	22.8	<i>Pantoea</i>	22.6	<i>Vibrio</i>	21.1	<i>Vibrio</i>	21.4
<i>Pantoea</i>	14.6	<i>Pantoea</i>	16.7			<i>Exiguoba cterium</i>	14.7	<i>Pantoea</i>	16	<i>Pantoea</i>	14.4
<i>Exiguoba cterium</i>	12.7	<i>Ralstonia</i>	13.6	<i>Erythrobacter</i>	20.3			<i>Exiguobacterium</i>	11.9	<i>Ralstonia</i>	11.3
<i>Erythrobacter</i>	10.6	<i>Erythrobacter</i>	11.1	<i>Alteromonas</i>	11.4	<i>Ralstonia</i>	13.2	<i>Alteromonas</i>	9.75	<i>Alteromonas</i>	10.0
<i>Pseudomonas</i>	6.99	<i>Exiguobacterium</i>	8.86	<i>Cycloclasticus</i>	8.77	<i>Pseudomonas</i>	9.29	<i>Pseudomonas</i>	7.5	<i>Exiguobacterium</i>	7.60
<i>Cycloclasticus</i>	4.72	<i>Cycloclasticus</i>	4.66	<i>Idiomarina</i>	5.26	<i>Dasania</i>	6.40				
<i>Pseudoruegeria</i>	3.77	<i>Pseudoruegeria</i>	3.68	<i>Idiomarina</i>	4.40	<i>Sphingobium</i>	3.97	<i>Idiomarina</i>	4.63	<i>Dasania</i>	5.41
<i>Sphingobium</i>	3.70	<i>Alteromonas</i>	3.48	<i>Pseudoalteromonas</i>	4.10	<i>Erythrobacter</i>	3.90	<i>Sphingobium</i>	4.52	<i>Idiomarina</i>	4.67
<i>Alteromonas</i>	2.96	<i>Caulobacter</i>	3.08	<i>Pseudoruegeria</i>	3.78	<i>Cycloclasticus</i>	3.49	<i>Pseudoalteromonas</i>	4.31	<i>Pseudoalteromonas</i>	4.35
<i>Brevundimonas</i>	2.44	<i>Marinobacter</i>	2.32	<i>Exiguobacterium</i>	3.59	<i>Caulobacter</i>	3.26	<i>Brevundimonas</i>	2.72	<i>Erythrobacter</i>	3.33
<i>Gilvibacter</i>	2.19	<i>Gilvibacter</i>	2.27			<i>Brevundimonas</i>	3.18	<i>Sphingomonas</i>	2.07	<i>Caulobacter</i>	2.75
<i>Marinobacter</i>	2.10			<i>Pantoea</i>	3.33	<i>Enhydrobacter</i>	2.49			<i>Cycloclasticus</i>	2.49
				<i>Gilvibacter</i>	2.16	<i>Sphingomonas</i>	2.41			<i>Sphingobium</i>	2.06
						<i>Massilia</i>	2.04				

**Table 4.** The contribution of particular eukaryotic taxa towards the total dissimilarity (in per cent) between the bacterial communities using similarity percentage (SIMPER) analysis. Groups with contribution  $\geq 2\%$  are shown.

Paint vs. Control		Paint vs. Base		Paint vs. Seawater		Control vs. Base		Control vs. Seawater		Base vs. Seawater	
Taxon	Contrb. %	Taxon	Contrb. %	Taxon	Contrb. %	Taxon	Contrb. %	Taxon	Contrb. %	Taxon	Contrb. %
<i>Bacillariophyceae</i>	21.5	<i>Hydrozoa</i>	25.05	<i>Bacillariophyceae</i>	22.56	<i>Bacillariophyceae</i>	26.43	<i>Bacillariophyceae</i>	26.43	<i>Hydrozoa</i>	25.49
<i>Hydrozoa</i>	16.81	<i>Ichthyosporea</i>	23.77	<i>Ichthyosporea</i>	18.18	<i>Hydrozoa</i>	25.54	<i>Dothideomycetes</i>	15.02	<i>Bacillariophyceae</i>	25.41
<i>Ichthyosporea</i>	16.25	<i>Agaricomycetes</i>	16.74	<i>Agaricomycetes</i>	14.51	<i>Dothideomycetes</i>	13.89	<i>Hydrozoa</i>	12.18	<i>Ichthyosporea</i>	10.02
<i>Agaricomycetes</i>	13.92	<i>Bacillariophyceae</i>	16.39	<i>Hydrozoa</i>	14.31	<i>Ichthyosporea</i>	9.358	<i>Agaricomycetes</i>	8.322	<i>Agaricomycetes</i>	6.903
<i>Dothideomycetes</i>	12	<i>Mediophyceae</i>	4.042	<i>Chlorophyta</i>	6.706	<i>Chlorophyta</i>	6.921	<i>Dinophyceae</i>	5.238	<i>Maxillopoda</i>	4.522
<i>Chlorophyta</i>	5.508	<i>Sordariomycetes</i>	2.538	<i>Dinophyceae</i>	4.657	<i>Mediophyceae</i>	3.704	<i>Trebouxioophyceae</i>	4.607	<i>Trebouxioophyceae</i>	4.271
<i>Dinophyceae</i>	2.245	<i>Maxillopoda</i>	2.063	<i>Maxillopoda</i>	4.316	<i>Dinophyceae</i>	2.537	<i>Maxillopoda</i>	4.035	<i>Mediophyceae</i>	4.04
<i>Sordariomycetes</i>	2.242			<i>Trebouxioophyceae</i>	3.754	<i>Agaricomycetes</i>	2.293	<i>Bangiophyceae</i>	2.299	<i>Bangiophyceae</i>	2.305
				<i>Sordariomycetes</i>	2.52			<i>Arachnida</i>	2.027	<i>Arachnida</i>	2.083
				<i>Bangiophyceae</i>	2.049						

## Supplementary

**Figure S1.** Vertical profiles of mean values of **A:** temperature, **B:** salinity, **C:** fluorescence intensity ( $\lambda=695\text{nm}$ ) and **D:** oxygen concentrations ( $\mu\text{mol kg}^{-1}$ ) during the period of investigations. The data plotted until the depth of 650m, as measured parameters did not change after that depth. Dashed curves represented minimal and maximal values.

